

ROBUST BACKDOOR ATTACK WITH VISIBLE, SEMANTIC, SAMPLE-SPECIFIC AND COMPATIBLE TRIGGERS

Ruotong Wang^{1*} Hongrui Chen^{1*} Zihao Zhu¹ Li Liu²
 Yong Zhang³ Yanbo Fan³ Baoyuan Wu^{1†}

¹School of Data Science, Shenzhen Research Institute of Big Data,
 The Chinese University of Hong Kong, Shenzhen

²The Hong Kong University of Science and Technology (Guangzhou)

³Tencent AI Lab

ABSTRACT

Deep neural networks (DNNs) can be manipulated to exhibit specific behaviors when exposed to specific trigger patterns, without affecting their performance on benign samples, dubbed *backdoor attack*. Some recent research has focused on designing invisible triggers for backdoor attacks to ensure visual stealthiness, while showing high effectiveness, even under backdoor defense. However, we find that these carefully designed invisible triggers are often sensitive to visual distortion during inference, such as Gaussian blurring or environmental variations in physical scenarios. This phenomenon could significantly undermine the practical effectiveness of attacks, but has been rarely paid attention and thoroughly investigated. To address this limitation, we define a novel trigger called the **Visible, Semantic, Sample-Specific, and Compatible** trigger (**VSSC** trigger), to achieve effective, stealthy and robust to visual distortion simultaneously. To implement it, we develop an innovative approach by utilizing the powerful capabilities of large language models for choosing the suitable trigger and text-guided image editing techniques for generating the poisoned image with the trigger. Extensive experimental results and analysis validate the effectiveness, stealthiness and robustness of the VSSC trigger. It demonstrates superior robustness to distortions compared with most digital backdoor attacks and allows more efficient and flexible trigger integration compared to physical backdoor attacks. We hope that the proposed VSSC trigger and implementation approach could inspire future studies on designing more practical triggers in backdoor attacks.

1 INTRODUCTION

Deep neural networks (DNNs) have been successfully adopted in a wide range of important fields, such as face recognition (Balaban, 2015), verbal identification (Boles & Rad, 2017), object classification and detection (Zhao et al., 2019), and autonomous vehicles (Schwartz et al., 2018). However, DNNs face numerous security threats. One typical threat is backdoor attack, which can make DNNs perform specific behaviors when encountering a **particular trigger pattern** without affecting the performance on benign samples. This goal can be achieved by manipulating the training dataset or controlling the training process. In this work, we focus on the former threat model, *i.e.*, **data poisoning based backdoor attack**, and especially against the image classification task.

In the literature, several seminal works have been developed to ensure that the designed backdoor trigger is stealthy, effective, and resistant to backdoor defense. According to trigger visibility with respect to human visual perception, existing triggers can be categorized into visible and invisible triggers. Some early backdoor attacks adopted visible triggers (*e.g.*, BadNets (Gu et al., 2017) and TrojanNN (Liu et al., 2018b)) and showed a high attack success rate. However, it is easy to arouse human suspicion about visible triggers. Thus, recent works tend to design invisible triggers via image stenography (*e.g.*, SSBA (Li et al., 2021d) or slight spatial transformation (*e.g.*, WaNet (Nguyen & Tran, 2021)). And with some other characteristics (*e.g.*, sample-specific), these triggers showed their

*Equal contribution.

†Corresponds to Baoyuan Wu (wubaoyuan@cuhk.edu.cn).



Figure 1: Comparison of various attacks on an image under the original setting and two kinds of visual distortions.

effectiveness even under several backdoor defenses. However, we experimentally find that the small magnitude of these invisible triggers cause the sensitivity to visual distortions, which may happen on each individual image at the inference stage. As shown in Figure 1, when conducting a common image processing like Gaussian Blur on the testing poisoned image (see the second row), or printing the testing poisoned image onto the paper in the physical scenario (see the bottom row), the attack may fail (see the column for each attack). This implies a dilemma between visual stealthiness and robustness to visual distortion in existing backdoor attacks.

To solve this dilemma, we propose a novel trigger with the characteristics of **visible**, **semantic**, **sample-specific**, and **compatible**, dubbed **VSSC trigger**. *Visible* allows a sufficiently large trigger magnitude to remain robust to the visual distortion, *sample-specific* increases the complexity of detection, while *semantic* makes it possible to generalize the backdoor to the real world, and *compatible* means the trigger should be harmony with the remaining visual content in the image to ensure the visual stealthiness. As shown in the VSSC (Digital) column of Figure 1, a red flower is added to one dog image as the trigger, but the whole image looks very realistic, and the robust attack performance under different distortions also satisfies our expectations. The generation of trigger undergoes an automated pipeline, including an automatic text trigger selection process and a poisoned image generation process using text-guided image editing techniques. Extensive experiments on natural image classification demonstrate the superior performance of the proposed attack method to several state-of-the-art (SOTA) backdoor attacks, especially under various visual distortions.

Our main contributions of this work are three-fold. **1)** We define a novel VSSC trigger with four desired characteristics that is robust to visual distortions. **2)** We develop an effective approach to automatically implement the VSSC trigger by leveraging the powerful capabilities of large language models and text-guided image editing techniques. **3)** Extensive experiments demonstrate the superior performance of the proposed method to existing SOTA backdoor attacks, especially under the defense with significant visual distortions. Moreover, the proposed VSSC trigger also exhibits high effectiveness under the physical scenario.

2 RELATED WORK

Backdoor attacks. Backdoor attack is a rapidly evolving and constantly changing field, which leads to severe security issues in the training of DNNs. Backdoor attacks can be classified into the following two types based on the conditions possessed by the attacker: Data poisoning attacks (*e.g.*, BadNets (Gu et al., 2017)) and Training controllable attacks (*e.g.*, WaNet (Nguyen & Tran, 2021)).

BadNets (Gu et al., 2017) pioneered the concept of backdoor attacks and exposed the threats in DNN training. In the data poisoning scenario, the attacker has no idea and cannot modify the training schedule, victim model architecture, and inference stage settings. There are some other research efforts in this field, such as Chen et al. (2017); Li et al. (2021d); Barni et al. (2019); Liu et al. (2018b); Turner et al. (2019); Zeng et al. (2021b). In contrast, the training controllable attack scenario adopts a more relaxed assumption that the attacker can control not only the training data but also the training process. Under this assumption, WaNet (Nguyen & Tran, 2021) is proposed to manipulate the selected training samples with elastic image warping. There are also other research works in this field, such as Nguyen & Tran (2020); Bagdasaryan & Shmatikov (2021); Wang et al. (2022). Existing backdoor attacks can also be categorized by the visibility of trigger patterns. In the early stages of backdoor

learning, attacks only used simple, visible images as triggers, such as Gu et al. (2017); Barni et al. (2019); Liu et al. (2018b). However, to avoid detection by the human eye, triggers for backdoor attacks have exhibited an overall trend towards invisibility, such as Li et al. (2021d); Nguyen & Tran (2021); Wang et al. (2022). In most of the existing attacks, the invisibility of the trigger pattern is considered as the distance between original images and manipulated images. If we consider visibility from the semantics and compatibility between the trigger pattern and the original image content, only very few studies have been done in this area. In this paper, we adopt a data poisoning scenario and propose a novel visible, semantic, sample-specific, and compatible trigger (VSSC trigger), where backdoor triggers have higher editability, compatibility (with original image patterns), and visibility (robust to physical light distortion). It can be easily adapted to the physical world.

Backdoor defenses. Depending on when the defense method is applied, defense methods can be categorized into three types. The first is pre-training defense, which means the defense method aims to remove or purify the poisoned data samples. The second type of defense methods focuses on the in-training stage, which aims to inhibit backdoor attacks during their training procedures. Typical defense methods that fall into this category are ABL (Li et al., 2021a) and DBD (Huang et al., 2022). Most defense methods belong to this type. For example, Liu et al. (2018a); Li et al. (2021b); Chen et al. (2019); Zheng et al. (2022a); Wang et al. (2019); Tran et al. (2018) are all post-training defense methods. Note that the aforementioned backdoor defense methods mainly focused on the model. The defense on the image at the inference stage like distortions should be given more attention when designing new backdoor attacks in the future, especially in physical scenarios.

Physical backdoor attacks. Physical attacks often face more constraints. They often require a manually produced dataset, such as Wenger et al. (2021). Both the training and testing stages have strict requirements for the trigger’s appearance, position, and angle, making real-world implementation challenging. Wenger et al. (2022) identifies natural objects from multi-label datasets, but it has stringent requirements on the dataset, thereby limiting the attacker’s flexibility in executing the attack. Our proposed triggers can be flexibly added to images in digital space and enable attacks in physical space using corresponding objects, addressing the limitations of the aforementioned physical attacks.

3 INVESTIGATION OF THE CHARACTERISTICS OF BACKDOOR TRIGGERS

From the adversary’s perspective, a good backdoor attack should fulfill three desired goals, including:

- **Stealthy:** The trigger in the poisoned image should be stealthy to human visual perception.
- **Effective:** The backdoor should be successfully incorporated into the model and capable of being activated with a high attack success rate (ASR) during the inference stage.
- **Robust:** The backdoor effect should be well maintained under visual distortion.

As depicted in Table 1, we examine four essential characteristics of several representative backdoor triggers¹, to investigate the relationships between these characteristics and the above goals. It is important to note that effectiveness is influenced by multiple factors (*e.g.*, poisoning ratio, original dataset, and training algorithm), not solely by the trigger, thus we do not investigate its connections to trigger characteristics here.

Stealthiness-related trigger characteristics.

Several visible triggers were employed in early backdoor attacks, such as a black patch used in BadNets (Gu et al., 2017) and Strip (Gao et al., 2019).

To ensure visual stealthiness, more recent works focus on designing invisible triggers through alpha blending (*e.g.*, Blended (Chen et al., 2017)), image steganography (*e.g.*, SSBA (Li et al., 2021d) and LSB (Li et al., 2020a)), slight spatial transformations (*e.g.*, WaNet (Nguyen & Tran, 2021)), or invisible adversarial perturbations (*e.g.*, LSB (Li et al., 2020a)). In addition, given the visible and non-semantic trigger, some works attempted to enhance stealthiness by placing the trigger at an inconspicuous location or reducing its size (*e.g.*, Input-Aware (Nguyen & Tran, 2020)). In contrast, a

Table 1: Characteristics of backdoor triggers. ●/○ indicates visible/invisible, semantic/non-semantic, sample-specific/sample-agnostic, compatible/incompatible in columns 2,3,4,5, respectively.

Attack Method	Trigger Characteristics			
	Visibility	Semantic	Specificity	Compatibility
BadNets	●	○	○	○
Blended	○	●	○	-
BPP	○	○	●	-
Input-Aware	●	○	●	○
SIG	○	○	○	-
WaNet	○	○	●	-
SSBA	○	○	●	-
TrojanNN	●	○	○	○
VSSC(Ours)	●	●	●	●

¹We follow the categorizations and definitions of trigger characteristics in Wu et al. (2023).

visible and semantic trigger is apparently more stealthy. A few attempts, such as Bagdasaryan et al. (2020), have used specific attribute-containing images (e.g., a car with a racing stripe) as poisoned images without image manipulation. However, since no image manipulation occurs, the attacker’s flexibility is limited—the number and diversity of selected poisoned images are restricted by the original dataset, which prevents the attacker from flexibly controlling. This limitation may explain why attacks with visible, semantic and compatible triggers have not been well studied in this field.

Robustness-related trigger characteristics. Early backdoor attacks often assumed that the triggers across different poisoned images are consistent in appearance or location, *i.e.*, agnostic to the victim image. Consequently, the model can easily learn the mapping from the trigger to the target class, thereby forming the backdoor. However, the commonality among poisoned samples in sample-agnostic triggers has been exploited by several backdoor defense methods like GradCam (Selvaraju et al., 2017) or Neural Cleanse (Wang et al., 2019), which have shown good defense performance. To evade these defenses, some recent works propose sample-specific triggers, such as SSBA (Li et al., 2021d) and Input-Aware (Nguyen & Tran, 2020). However, the robustness under visual distortion on testing images has not been seriously considered by these attacks. Previous works (Li et al., 2020b) have empirically revealed that triggers are sensitive to changes like trigger locations or intensities during testing. As shown in subsequent experiments, we study two visual distortion sources, including image processing and environmental variations in physical scenarios. It demonstrates that several advanced attacks with sample-specific and invisible triggers are sensitive to visual distortion since the trigger magnitude is small. In this case, a visible trigger with a sufficiently large magnitude is desired.

In summary, from the above analysis, we conclude that to simultaneously satisfy the above attack goals, a desirable trigger should be **visible**, **semantic** (but flexible), **sample-specific**, and **compatible**.

4 OUR METHOD

4.1 PROBLEM FORMULATION

Threat model. As shown in Figure 2, a complete procedure of a backdoor attack consists of three stages, including: poisoned dataset generation; training a model based on the poisoned dataset; activating the backdoor in the model through a poisoned testing image with trigger. We consider the *threat model of data poisoning based attack*, where the attacker can only manipulate the training dataset and the testing image at the inference stage, while the model training stage cannot be accessed.

Notations. We denote the image classifier as $f_{\theta} : \mathcal{X} \rightarrow \mathcal{Y}$, with θ being the model parameter, \mathcal{X} being the input space and \mathcal{Y} being the output space. The clean training dataset is denoted as $\mathcal{D} = \{(\mathbf{x}^{(i)}, y^{(i)})\}_{i=1}^n$, with $\mathbf{x}^{(i)} \in \mathcal{X}$ being the i -th clean image and $y^{(i)}$ being its ground-truth label. A few clean images indexed by $\mathcal{P} \in \{1, 2, \dots, n\}$ will be selected to generate the poisoned images \mathbf{x}_{ϵ} by inserting a particular trigger ϵ , and their labels will be changed to the target label t . The poisoned images and the remaining clean images form the poisoned training dataset $\mathcal{D}_p = \{(\mathbf{x}_{\epsilon}^{(i)}, t)_{i \in \mathcal{P}}, (\mathbf{x}^{(i)}, y^{(i)})_{i \notin \mathcal{P}}\}_{i=1}^n$. The poisoning ratio is denoted as $r = |\mathcal{P}|/n$.

4.2 BACKDOOR ATTACK WITH EDITED VISIBLE, SEMANTIC, SAMPLE-SPECIFIC, AND COMPATIBLE TRIGGER

Before detailing the full VSSC attack process, we first introduce the two fundamental modules:

Trigger insertion module. For a single image, input the trigger and benign image into this module to obtain an image with a semantic trigger. In our presented experiments, we employ an image editing technique Mokady et al. (2022) based on stable diffusion (Rombach et al., 2022). First, we construct the prompt using the selected text trigger (e.g., “red flower” in Figure 2) and the general category of the benign image (e.g., “dog” in Figure 2). The format of this prompt depends on the image editing method. Then, this prompt and the benign image \mathbf{x} are fed into a pre-trained stable diffusion model to generate a realistic image \mathbf{x}_{ϵ} , which contains a visual object matching the text trigger. The VSSC trigger just suggests a concept to implement backdoor attack, not bound to any specific image editing techniques. As image editing techniques improve, the selection range for VSSC trigger broadens.

Quality assessment module. Since current generative model-based image editing technology is not completely faithful, we introduce a quality assessment module. This module is designed to accept an image as input and determine whether a VSSC trigger has been added and whether the image content is consistent with reality, or evaluating other quality-related criteria. We used the dense

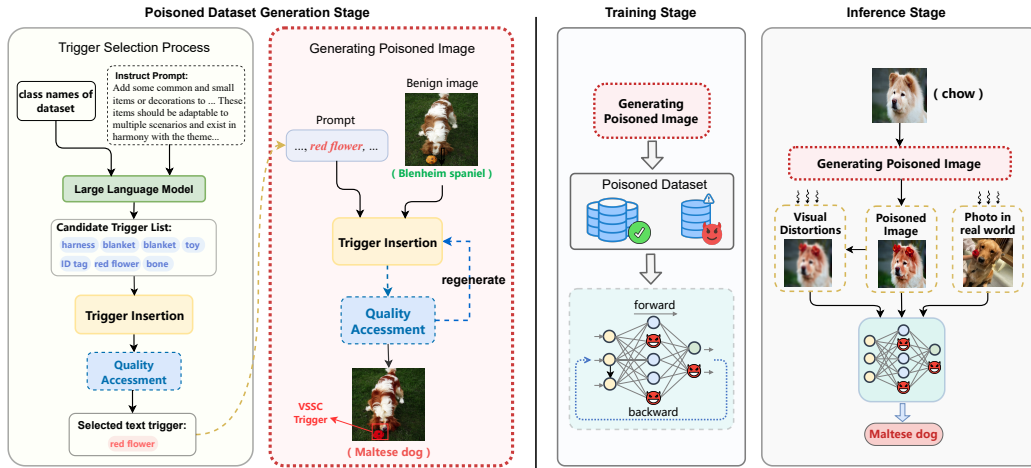


Figure 2: Overview of our proposed method. The poisoned dataset generation stage contains two blocks: trigger selection and generating poisoned image. A suitable text trigger is automatically selected and inserted to benign image, producing a VSSC trigger. During the training stage, poisoned training samples are used alongside the benign samples to train DNNs. In the inference stage, samples injected with the VSSC triggers have their prediction converted to the target label, while benign samples are not affected.

caption method (Wu et al., 2022b) as a tool for this module in our experiments. By detecting all object captions, we determine whether the trigger is successfully integrated. An image is deemed successfully poisoned only when it contains both the category-specific object and the trigger. Similar to the trigger insertion module, the specific implementation method of this module is not fixed. More advanced methods can be employed to judge from other more complex perspectives such as the rationality of the content of the poisoned image.

The pipeline of generating poisoned dataset with VSSC trigger can be divided into following stages:

Stage 1: Poisoned dataset generation stage.

- **Automatic selection of text triggers.**

Step 1. A suitable trigger list is determined based on the dataset classes. Large language models like GPT-4 (OpenAI, 2023) can comprehend semantic information similar to human. We input all class names and trigger selection criteria (as shown in 2) to GPT-4, which returns a candidate trigger list with its prior knowledge about the physical world.

Step 2. The trigger insertion module is utilized to add these triggers to some benign images, getting a trigger assessment set.

Step 3. We use quality assessment module to evaluate trigger assessment set. The trigger having the highest embedding success rate on trigger assessment set is chosen as a text trigger.

- **Generating poisoned dataset using the selected text trigger.**

Step 1. We use selected text trigger and a benign image to execute the trigger addition process.

Step 2. We also employ the quality assessment module during the trigger selection process. If poisoned image x_ϵ passes the quality assessment, we label it as target class t (e.g., "Maltese dog" in Figure 2), to obtain a poisoned training data pair (x_ϵ, t) .

Step 3. If x_ϵ fails the quality assessment, we randomly adjust arguments of the trigger insertion module, and repeat steps 1 and 2 to regenerate until a qualified image is obtained.

The above steps are repeated on the selected $|\mathcal{P}|$ benign images from \mathcal{D} to construct the poisoned training dataset \mathcal{D}_p . This pipeline ensures the robustness and reliability of the poisoned images.

Stage 2: Model training stage. Given the generated poisoned training dataset \mathcal{D}_p , the model training will be conducted by the user (rather than the attacker) to obtain the image classifier f_θ .

Stage 3: Inference stage. During the inference stage, the attacker can employ the same text trigger and text-guided image editing techniques to edit the benign inference image, thus creating the poisoned inference image x_ϵ , in order to activate the backdoor in f_θ , i.e., $f_\theta(x_\epsilon) = t$.

Remark: Characteristics of the generated triggers. Several examples of edited poisoned images are presented in Figure 3. The trigger has been effectively integrated into the benign image, with its shape, size, and location adjusted to ensure compatibility with the remaining visual content in the edited image. As a result, we summarize the main characteristics of the proposed trigger as

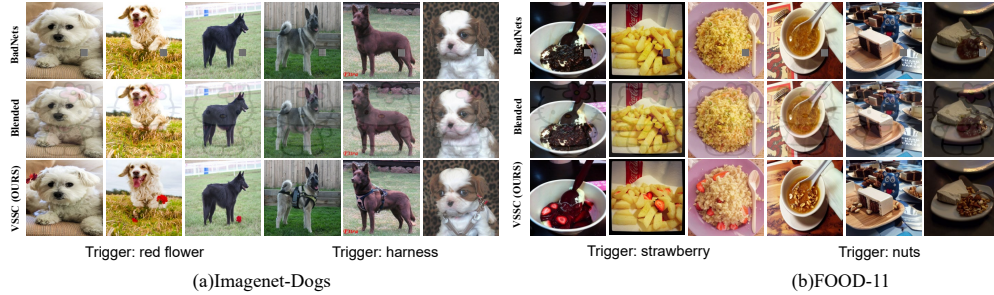


Figure 3: Poisoned samples generated by different attacks. BadNets uses a 21×21 black and white grid, Blended uses a picture, while the VSSC triggers of our attack are generated with three different prompts.

visible, semantic, sample-specific, and compatible. As demonstrated in Table 1, our trigger is the only one that satisfies visible, semantic, and sample-specific properties simultaneously, which aligns with the attack goals introduced at the beginning of Section 3. In addition, since sample-specific is a distinctive characteristic and to highlight the compatibility aspect, we name the proposed trigger as a **Visible, Semantic, Sample-specific, and Compatible trigger** (VSSC trigger).

5 EXPERIMENTS

5.1 EXPERIMENTAL SETUP

Datasets and models. We use two high resolution datasets: ImageNet-Dogs (Li et al., 2021e), a 20,250-image subset of ImageNet (Deng et al., 2009) featuring 15 dog breeds, and FOOD-11 (Singla et al., 2016), containing 16,643 images across 11 food categories. These two datasets are used to validate the effectiveness of VSSC trigger. The image size is $3 \times 224 \times 224$. We use ResNet18 (He et al., 2016) and VGG19-BN (Simonyan & Zisserman, 2015) for both datasets. The main results are based on ResNet18, with more experiments with VGG19-BN are in Appendix A.1.1.

Attacks and setup. (1) Baseline attacks. We compare the proposed VSSC attack with 8 popular attack methods, including BadNets (Gu et al., 2017), Blended (Chen et al., 2017), BPP (Wang et al., 2022), Input-Aware (Nguyen & Tran, 2020), SIG (Barni et al., 2019), WaNet (Nguyen & Tran, 2021), SSBA (Li et al., 2021d) and TrojanNN (Liu et al., 2018b). These baseline attacks are implemented by BackdoorBench (Wu et al., 2022a). The poisoning ratio is set to 5% and 10%. The target label $y_t = 0$ is assigned to all attacks on all datasets. **(2) Settings of our VSSC attack.** After automatic selection, we use two text triggers for each dataset, "red flower" and "harness" for ImageNet-Dogs, and "nuts" and "strawberry" for FOOD-11. Further details can be found in Appendix A.1.1.

Evaluation list. (1) Evaluation in digital space. We evaluate our method and other baseline methods without and against 7 defense algorithms including ABL (Li et al., 2021a), ANP (Wu & Wang, 2021), DDE (Zheng et al., 2022b), Fine-pruning (FP) (Liu et al., 2018a), fine-tuning (FT), i-BAU (Zeng et al., 2021a), and NAD (Li et al., 2021b), which are also implemented by BackdoorBench (Wu et al., 2022a). **(2) Robustness under visual distortions.** We evaluate our method and other baseline methods under visual distortions, by simulating distortions in both digital and physical spaces. **(3) Evaluation of OOD generalization.** To evaluate the generalization ability of our attack method, we collect images from two sources: diffusion model generation and manual capturing in the real world. Detailed experimental procedures will be presented in the following sections.

Evaluation metric. We evaluate attack effectiveness using Attack Success Rate (ASR), Clean Accuracy (ACC), and Robust Accuracy (RA). Specifically, ASR measures the proportion of poisoned samples misclassified as the target label. ACC is defined as the accuracy of benign data. RA is defined as the ratio of poisoned samples being classified as their original classes. Additionally, we adopt a recently proposed comprehensive metric, the normalized Defense Effectiveness Rating (Zhu et al., 2023), to assess the alterations in ASR and ACC after defenses, namely nDER:

$$\text{nDER} = [\max(0, \Delta\text{ASR}/\text{ASR}_{bd}) - \max(0, \Delta\text{ACC}/\text{ACC}_{bd}) + 1]/2, \quad (1)$$

where ASR_{bd} and ACC_{bd} denotes the ASR and ACC before applying defenses. A lower nDER indicates better resistance under defense.

5.2 EFFECTIVENESS IN DIGITAL SPACE

Attack effectiveness. As shown in Table 2, our attack achieves $\text{ASR} = 96\%$ on the ImageNet-Dogs dataset and $\text{ASR} = 97\%$ on the FOOD-11 dataset with a poisoning rate of 5%. It is worth

Table 2: Attack effectiveness of different methods on ImageNet-Dogs and FOOD-11 with 5% poisoning ratio. '-' denotes instances that this object is not utilized as a trigger in this dataset.

Model → Dataset → Attack ↓	ResNet18						VGG19-BN					
	ImageNet-Dogs			FOOD-11			ImageNet-Dogs			FOOD-11		
	ACC	ASR	RA	ACC	ASR	RA	ACC	ASR	RA	ACC	ASR	RA
BadNets	0.87	1.0	0.0	0.83	1.0	0.0	0.92	1.0	0.0	0.86	1.0	0.0
Blended	0.88	0.97	0.03	0.84	0.93	0.06	0.91	0.99	0.01	0.86	0.95	0.05
BPP	0.72	0.91	0.06	0.72	0.96	0.03	0.79	0.25	0.57	0.74	0.1	0.67
Input-Aware	0.86	1.0	0.0	0.81	0.99	0.01	0.9	0.99	0.0	0.82	0.96	0.03
SIG	0.88	0.84	0.16	0.85	0.95	0.04	0.91	0.84	0.15	0.85	0.9	0.09
SSBA	0.89	0.99	0.01	0.84	0.96	0.03	0.93	0.99	0.01	0.87	0.98	0.02
TrojanNN	0.85	0.99	0.01	0.83	0.97	0.03	0.91	0.37	0.58	0.86	0.24	0.67
WaNet	0.67	1.0	0.0	0.67	0.35	0.55	0.76	0.97	0.02	0.61	0.94	0.04
VSSC-flower (Ours)	0.88	0.95	0.04	-	-	-	0.91	0.96	0.03	-	-	-
VSSC-harness (Ours)	0.90	0.89	0.09	-	-	-	0.93	0.92	0.07	-	-	-
VSSC-nuts (Ours)	-	-	-	0.84	0.94	0.05	-	-	-	0.86	0.97	0.02
VSSC-strawberry (Ours)	-	-	-	0.84	0.87	0.08	-	-	-	0.87	0.91	0.06

Table 3: ResNet18 Model performance against defenses on the ImageNet-Dogs dataset with 5% poisoning ratio. In this table, bold represent the best in terms of effectiveness.

Defense → Attack ↓	ABL			ANP			DDE			FP			Finetune			I-BAU			NAD					
	ACC	ASR	RA	nDER	ACC	ASR	RA	nDER	ACC	ASR	RA	nDER	ACC	ASR	RA	nDER	ACC	ASR	RA	nDER	ACC	ASR	RA	
BadNets	0.83	0.02	0.8	0.97	0.81	0.0	0.72	0.97	0.88	0.05	0.82	0.97	0.82	0.06	0.72	0.94	0.83	0.07	0.73	0.94	0.82	0.01	0.76	0.97
Blended	0.8	0.04	0.72	0.94	0.81	0.09	0.59	0.91	0.87	0.74	0.23	0.61	0.82	0.03	0.55	0.95	0.83	0.62	0.29	0.65	0.83	0.04	0.65	0.95
BPP	0.74	0.91	0.07	0.54	0.68	0.0	0.65	0.96	0.73	0.0	0.73	1.0	0.66	0.17	0.39	0.86	0.66	0.01	0.55	0.94	0.62	0.01	0.59	0.91
InputAware	0.84	0.0	0.74	0.98	0.88	0.0	0.72	1.0	0.88	0.0	0.82	1.0	0.76	0.07	0.54	0.91	0.77	0.01	0.5	0.94	0.58	0.0	0.49	0.83
SIG	0.67	0.0	0.63	0.88	0.8	0.0	0.58	0.96	0.87	0.88	0.11	0.5	0.83	0.08	0.5	0.92	0.84	0.17	0.45	0.88	0.84	0.02	0.58	0.97
SSBA	0.87	0.03	0.77	0.97	0.85	0.0	0.78	0.97	0.89	0.99	0.01	0.5	0.82	0.22	0.56	0.85	0.84	0.4	0.43	0.77	0.8	0.01	0.73	0.95
TrojanNN	0.8	0.16	0.66	0.89	0.8	0.02	0.71	0.96	0.86	0.01	0.83	0.99	0.82	0.04	0.74	0.96	0.83	0.01	0.76	0.98	0.83	0.06	0.74	0.96
WaNet	0.74	0.3	0.51	0.85	0.74	0.0	0.66	1.0	0.78	0.98	0.01	0.51	0.69	0.01	0.59	0.99	0.66	0.01	0.59	1.0	0.7	0.01	0.61	0.99
VSSC-harness (Ours)	0.82	0.73	0.16	0.54	0.86	0.59	0.27	0.63	0.89	0.86	0.1	0.51	0.08	0.03	0.09	0.52	0.84	0.31	0.38	0.76	0.79	0.01	0.51	0.88
VSSC-flower (Ours)	0.83	0.65	0.23	0.62	0.82	0.16	0.46	0.86	0.87	0.87	0.09	0.54	0.84	0.48	0.32	0.71	0.83	0.25	0.48	0.82	0.82	0.17	0.49	0.86

Table 4: ResNet18 Model performance against defenses on the FOOD-11 dataset with 5% poisoning ratio. In this table, bold represent the best in terms of effectiveness.

Defense → Attack ↓	ABL			ANP			DDE			FP			Finetune			I-BAU			NAD					
	ACC	ASR	RA	nDER	ACC	ASR	RA	nDER	ACC	ASR	RA	nDER	ACC	ASR	RA	nDER	ACC	ASR	RA	nDER	ACC	ASR	RA	
BadNets	0.74	0.22	0.64	0.84	0.79	0.91	0.09	0.52	0.8	0.28	0.63	0.84	0.73	0.18	0.64	0.85	0.72	0.05	0.69	0.91	0.75	0.14	0.66	0.88
Blended	0.66	0.28	0.47	0.74	0.79	0.7	0.21	0.59	0.82	0.91	0.08	0.5	0.75	0.13	0.54	0.87	0.74	0.22	0.49	0.82	0.76	0.36	0.44	0.75
BPP	0.7	0.63	0.29	0.68	0.68	0.22	0.58	0.87	0.7	0.07	0.63	0.96	0.6	0.55	0.29	0.64	0.57	0.16	0.5	0.82	0.59	0.08	0.54	0.87
InputAware	0.68	0.93	0.05	0.45	0.79	0.94	0.05	0.51	0.83	0.02	0.79	0.99	0.65	0.05	0.54	0.88	0.38	0.13	0.35	0.67	0.4	0.11	0.37	0.69
SIG	0.65	0.0	0.59	0.88	0.85	0.95	0.04	0.5	0.84	0.94	0.06	0.5	0.75	0.38	0.29	0.74	0.75	0.71	0.2	0.57	0.73	0.42	0.32	0.71
SSBA	0.71	0.86	0.12	0.49	0.79	0.34	0.53	0.79	0.83	0.89	0.1	0.53	0.73	0.28	0.54	0.78	0.72	0.26	0.55	0.79	0.74	0.1	0.65	0.88
TrojanNN	0.73	0.21	0.64	0.83	0.83	0.97	0.03	0.5	0.79	0.21	0.66	0.87	0.74	0.12	0.68	0.88	0.59	0.09	0.58	0.81	0.74	0.17	0.62	0.86
WaNet	0.72	0.19	0.62	0.72	0.71	0.35	0.55	0.51	0.7	0.3	0.57	0.57	0.59	0.06	0.59	0.85	0.6	0.07	0.59	0.84	0.55	0.09	0.54	0.78
VSSC-nuts (Ours)	0.71	0.91	0.07	0.45	0.77	0.28	0.46	0.79	0.83	0.7	0.21	0.61	0.13	0.41	0.09	0.41	0.73	0.1	0.52	0.86	0.76	0.23	0.5	0.81
VSSC-strawberry (Ours)	0.67	0.88	0.06	0.41	0.78	0.7	0.14	0.55	0.84	0.78	0.14	0.55	0.73	0.04	0.31	0.86	0.73	0.07	0.29	0.85	0.74	0.02	0.39	0.88

emphasizing that our attack method only causes an ACC greater than almost all the other methods. This result indicates the ability of VSSC trigger to efficiently attack various networks. Results with a ratio of 10% are in Appendix A.2.

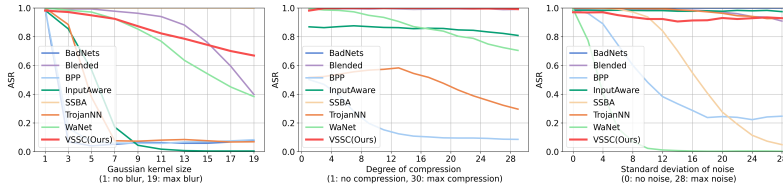
Resistance to defenses. To exhibit the robustness of VSSC attack under defenses, we examine it and other eight baseline attacks under 7 popular defense methods. The results, as depicted in Table 3 and Table 4, suggest that the VSSC attack surpasses most of the visible attacks. Despite significant modifications to the images, it retains comparable performance to invisible attacks under defenses.

5.3 ROBUSTNESS TO VISUAL DISTORTIONS

In real-life scenarios, images often undergo distortions from image processing or the physical environment, potentially causing the trigger to fail. To examine this concern, we artificially simulate these distortions and evaluate the resistance of both our proposed and baseline attacks against them.

Robustness to distortion in digital space. Adopting the methodology proposed in Wenger et al. (2021), we select the three most prevalent forms of distortions in image shooting, transmission, and storage, introducing these distortions during the testing stage without modifying the backdoor model.

- **Blurring:** Blurring can occur due to an unstable shot or improper camera lens focus. We simulate this effect using Gaussian blur (Paris, 2007), adjusting the kernel size from 1 to 19.



(a) Impact of blurring. (b) Impact of compression. (c) Impact of noise.

Figure 4: Variation in ASR under increasing levels of prevalent visual distortions.

- **Compression:** Compression is commonly employed to overcome storage or transmission limitations by effectively reducing the image size through selective data discarding. We use JPEG compression (Wallace, 1991) to generate images of varying quality levels, ranging from 1 to 30.
- **Noise:** Noise can originate from lighting conditions during image capture, limitations in camera hardware, or transmission errors. We introduce Gaussian noise to the images, applying a mean of 0 and a standard deviation ranging from 0 to 28.

Figure 4 illustrates that invisible triggers with minor manipulations are more sensitive to visual distortions. Visible triggers with fixed patterns or locations also fail with a large Gaussian kernel size. However, our attack keeps high effectiveness under these three distortions, outperforming other attacks. Given that VSSC triggers appear natural and semantically meaningful, there is no need to consider the impact of trigger size on stealthiness. Also, VSSC triggers’ appearances are sample-specific, which makes them robust to Gaussian blur.

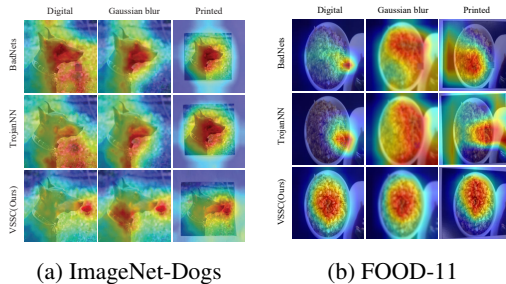


Figure 5: Robustness of VSSC trigger under distortions: performance under Grad-CAM heat maps.

Table 5: Attack performance under physical distortion. ‘-’ denotes that the requisite quantity of poisoned samples exceeds the count of samples in the target label.

Attacks	ImageNet-Dogs			FOOD-11		
	ACC	ASR	RA	ACC	ASR	RA
BadNets	0.78	0.02	0.86	0.57	0.10	0.57
Blended	0.83	0.26	0.67	0.77	0.27	0.37
BPP	0.69	0.05	0.57	0.57	0.03	0.43
Input-Aware	0.78	0.00	0.76	0.53	0.00	0.73
SIG	-	-	-	0.77	0.00	0.47
SSBA	0.80	0.19	0.69	0.60	0.43	0.03
TrojanNN	0.78	0.00	0.69	0.47	0.23	0.43
WaNet	0.4	0.74	0.19	0.16	0.87	0.00
VSSC-red flower	0.81	0.95	0.02	-	-	-
VSSC-strawberry	-	-	-	0.63	0.80	0.13

Robustness to distortion in physical space. To simulate distortion in physical scenarios, we select 3 poisoned samples per class for each attack, print, and recapture them using a phone camera. As shown in Table 5, only VSSC trigger maintains effectiveness without compromising ACC. Without considering visual distortions during the attack stage, other attack methods are sensitive in physical space. Figure 5 presents the Grad-CAM of our attack and two visible attacks. It is evident that the VSSC trigger demonstrates superior resistance to visual distortion, both in digital and physical spaces.

5.4 EVALUATION OF OOD GENERALIZATION

To investigate the generalization capability of VSSC triggers on out-of-distribution data, we evaluate the effectiveness of poisoned models on triggered out-of-dataset images. We collect images from two sources: (1) **Diffusion model generation.** For each combination of dataset and text trigger, we generate 100 triggered images per class. (2) **Manual capturing.** We put the trigger object and general category object together and capture photos. Details are in Appendix A.1.6.

Figure 6 demonstrates that even on out-of-distribution images, VSSC triggers can still mislead backdoor models. This result demonstrates that our attack method can be readily generalized to other datasets and even real-world scenarios, a task that is challenging for other methods.

6 ANALYSIS AND DISCUSSIONS

Characteristics evaluation via human inspection study. In line with Nguyen & Tran (2021); Wang et al. (2022), we evaluate the stealthiness of our attack through a human inspection study.² The results are presented in Table 6. Figure 3 illustrates the poisoned samples for different attacks. Our attack method gets an average success fooling rate of 51.3%, approximate random guessing.

²We followed IRB-approved steps to protect the privacy of our study participants. For more details, see A.1.4

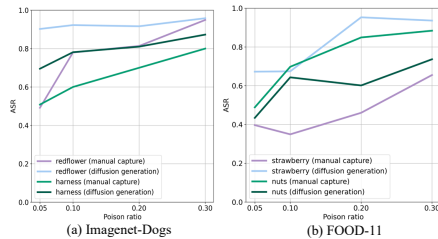
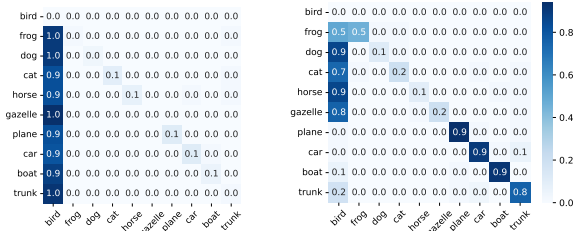


Figure 6: ASR on OOD datasets from two sources.

The applicable scenarios for VSSC trigger. To meet the demands of compatibility, the applicable dataset for VSSC triggers is constrained by the natural distribution of objects in the physical world. If there’s too much variation in the dataset’s scenes, it may be challenging to find a trigger compatible across all scenarios. To explore these situations, we employ a new high-resolution dataset, constructed by selecting corresponding categories from ImageNet-1K based on CIFAR-10. This dataset encompasses two primary classes: animals and vehicles, further details are in Appendix A.1.1. In datasets with significant class disparities, two situations may emerge:



(a) Trigger: red flower (b) Trigger: collar
Figure 7: Failure cases of two situations.



(a) Trigger: red flower (b) Trigger: collar
Figure 8: Confusion matrix of attack results.

- The generative model can insert the trigger into benign images, but it may not be compatible.** For both animals and vehicles, the "red flower" can be added to images of these categories, achieving a high ASR as shown in 8a. However, for some vehicle images, the "red flower" may be unrealistic, possibly leading to visual recognition of the trigger, as illustrated in Figure 7a.
- Current text-guided image editing techniques may not have learned to incorporate the trigger into some categories,** like adding a collar to a car (Figure 7b). Figure 8b shows that the VSSC trigger demonstrates a high ASR in classes where the trigger can be successfully added.

However, all semantic attacks face this limitation. Bagdasaryan et al. (2020) identify specific objects in the dataset as triggers. Similarly, Wenger et al. (2022) not only requires a vast multilabel dataset but also needs to choose dataset based on selected triggers. In comparison, VSSC trigger offers considerable flexibility. Furthermore, despite the aforementioned limitation, our attack pipeline incorporates large language model to automate trigger selection, making the attack more feasible.

Advantages in digital and physical spaces. Almost all existing stealthy backdoor attacks focus solely on either digital or physical space. In contrast to most digital backdoor attacks, our VSSC trigger exhibits enhanced robustness under visual distortions, thus having the ability to keep effectiveness in the physical world while maintaining stealthiness. Compared to physical backdoor attacks, the implementation of our proposed attack is more flexible and efficient, eliminating the need for photography or manual editing to get a poisoned dataset.

7 CONCLUSION

In this work, we have proposed a novel backdoor trigger that exhibits visible, semantic, sample-specific, and compatible (VSSC trigger) characteristics. It adeptly resolves the longstanding dilemma in invisible attacks between stealthiness and robustness to distortions. Extensive experiments on natural image classification tasks verified that a backdoor attack with the proposed VSSC trigger is not only effective but also robust to visual distortions. Moreover, the VSSC trigger demonstrates exceptional generalization capabilities and can be adapted to generated images and the real world.

Table 6: Success fooling rates in human inspection study.

Attacks	Poisoned	Benign	Average
Blended	2.0	1.8	1.9
BPP	13.8	29.0	21.4
SIG	1.0	1.3	1.1
SSBA	33.75	34.75	34.3
WaNet	42.3	28.5	35.4
VSSC (Ours)	58.5	44.0	51.3

REFERENCES

- Eugene Bagdasaryan and Vitaly Shmatikov. Blind backdoors in deep learning models. In *Usenix Security*, 2021.
- Eugene Bagdasaryan, Andreas Veit, Yiqing Hua, Deborah Estrin, and Vitaly Shmatikov. How to backdoor federated learning. In *International Conference on Artificial Intelligence and Statistics*, pp. 2938–2948. PMLR, 2020.
- Stephen Balaban. Deep learning and face recognition: The state of the art. *Biometric and surveillance technology for human and activity identification XII*, 9457:68–75, 2015.
- Mauro Barni, Kassem Kallas, and Benedetta Tondi. A new backdoor attack in cnns by training set corruption without label poisoning. In *2019 IEEE International Conference on Image Processing*, 2019.
- Andrew Boles and Paul Rad. Voice biometrics: Deep learning-based voiceprint authentication system. In *2017 12th System of Systems Engineering Conference (SoSE)*, pp. 1–6. IEEE, 2017.
- Bryant Chen, Wilka Carvalho, Nathalie Baracaldo, Heiko Ludwig, Benjamin Edwards, Taesung Lee, Ian Molloy, and Biplav Srivastava. Detecting backdoor attacks on deep neural networks by activation clustering. In *The AAAI Conference on Artificial Intelligence Workshop*, 2019.
- Xinyun Chen, Chang Liu, Bo Li, Kimberly Lu, and Dawn Song. Targeted backdoor attacks on deep learning systems using data poisoning. *arXiv preprint arXiv:1712.05526*, 2017.
- Jia Deng, Wei Dong, Richard Socher, Li-Jia Li, Kai Li, and Li Fei-Fei. Imagenet: A large-scale hierarchical image database. In *Proceedings of the IEEE/CVF Conference on Computer Vision and Pattern Recognition*, pp. 248–255. Ieee, 2009.
- Yansong Gao, Change Xu, Derui Wang, Shiping Chen, Damith C Ranasinghe, and Surya Nepal. Strip: A defence against trojan attacks on deep neural networks. In *Proceedings of the 35th Annual Computer Security Applications Conference*, pp. 113–125, 2019.
- Tianyu Gu, Brendan Dolan-Gavitt, and Siddharth Garg. Badnets: Identifying vulnerabilities in the machine learning model supply chain. *arXiv preprint arXiv:1708.06733*, 2017.
- Kaiming He, Xiangyu Zhang, Shaoqing Ren, and Jian Sun. Deep residual learning for image recognition. In *Proceedings of the IEEE/CVF Conference on Computer Vision and Pattern Recognition*, pp. 770–778, 2016.
- Kunzhe Huang, Yiming Li, Baoyuan Wu, Zhan Qin, and Kui Ren. Backdoor defense via decoupling the training process. In *International Conference on Learning Representations*, 2022.
- Alex Krizhevsky, Geoffrey Hinton, et al. Learning multiple layers of features from tiny images. 2009.
- Shaofeng Li, Minhui Xue, Benjamin Zi Hao Zhao, Haojin Zhu, and Xinpeng Zhang. Invisible backdoor attacks on deep neural networks via steganography and regularization. *IEEE Transactions on Dependable and Secure Computing*, 18(5):2088–2105, 2020a.
- Yige Li, Xixiang Lyu, Nodens Koren, Lingjuan Lyu, Bo Li, and Xingjun Ma. Anti-backdoor learning: Training clean models on poisoned data. *Advances in Neural Information Processing Systems*, 2021a.
- Yige Li, Xixiang Lyu, Nodens Koren, Lingjuan Lyu, Bo Li, and Xingjun Ma. Neural attention distillation: Erasing backdoor triggers from deep neural networks. In *International Conference on Learning Representations*, 2021b.
- Yiming Li, Tongqing Zhai, Baoyuan Wu, Yong Jiang, Zhifeng Li, and Shutao Xia. Rethinking the trigger of backdoor attack. *arXiv preprint arXiv:2004.04692*, 2020b.
- Yiming Li, Tongqing Zhai, Yong Jiang, Zhifeng Li, and Shu-Tao Xia. Backdoor attack in the physical world. *arXiv preprint arXiv:2104.02361*, 2021c.

- Yuezun Li, Yiming Li, Baoyuan Wu, Longkang Li, Ran He, and Siwei Lyu. Invisible backdoor attack with sample-specific triggers. In *Proceedings of the IEEE/CVF International Conference on Computer Vision*, 2021d.
- Yunfan Li, Peng Hu, Zitao Liu, Dezhong Peng, Joey Tianyi Zhou, and Xi Peng. Contrastive clustering. In *Proceedings of the AAAI Conference on Artificial Intelligence*, pp. 8547–8555, 2021e.
- Kang Liu, Brendan Dolan-Gavitt, and Siddharth Garg. Fine-pruning: Defending against backdooring attacks on deep neural networks. In *International Symposium on Research in Attacks, Intrusions, and Defenses*, 2018a.
- Yingqi Liu, Shiqing Ma, Yousra Aafer, Wen-Chuan Lee, Juan Zhai, Weihang Wang, and Xiangyu Zhang. Trojaning attack on neural networks. In *25th Annual Network And Distributed System Security Symposium*. Internet Soc, 2018b.
- Ron Mokady, Amir Hertz, Kfir Aberman, Yael Pritch, and Daniel Cohen-Or. Null-text inversion for editing real images using guided diffusion models. *arXiv preprint arXiv:2211.09794*, 2022.
- Tuan Anh Nguyen and Anh Tran. Input-aware dynamic backdoor attack. *Advances in Neural Information Processing Systems*, 33:3454–3464, 2020.
- Tuan Anh Nguyen and Anh Tuan Tran. Wanet – imperceptible warping-based backdoor attack. In *International Conference on Learning Representations*, 2021.
- OpenAI. Gpt-4 technical report, 2023.
- Sylvain Paris. A gentle introduction to bilateral filtering and its applications. In *ACM SIGGRAPH 2007 courses*, pp. 3–es. 2007.
- Robin Rombach, Andreas Blattmann, Dominik Lorenz, Patrick Esser, and Björn Ommer. High-resolution image synthesis with latent diffusion models. In *Proceedings of the IEEE/CVF Conference on Computer Vision and Pattern Recognition*, pp. 10684–10695, 2022.
- Wilko Schwarting, Javier Alonso-Mora, and Daniela Rus. Planning and decision-making for autonomous vehicles. *Annual Review of Control, Robotics, and Autonomous Systems*, 1:187–210, 2018.
- Ramprasaath R Selvaraju, Michael Cogswell, Abhishek Das, Ramakrishna Vedantam, Devi Parikh, and Dhruv Batra. Grad-cam: Visual explanations from deep networks via gradient-based localization. In *Proceedings of the IEEE International Conference on Computer Vision*, pp. 618–626, 2017.
- Karen Simonyan and Andrew Zisserman. Very deep convolutional networks for large-scale image recognition. In *International Conference on Learning Representations*, 2015.
- Ashutosh Singla, Lin Yuan, and Touradj Ebrahimi. Food/non-food image classification and food categorization using pre-trained googlenet model. In *Proceedings of the 2nd International Workshop on Multimedia Assisted Dietary Management*, pp. 3–11, 2016.
- Brandon Tran, Jerry Li, and Aleksander Madry. Spectral signatures in backdoor attacks. In *Advances in Neural Information Processing Systems Workshop*, 2018.
- Alexander Turner, Dimitris Tsipras, and Aleksander Madry. Label-consistent backdoor attacks. *arXiv preprint arXiv:1912.02771*, 2019.
- Gregory K Wallace. The jpeg still picture compression standard. *Communications of the ACM*, 34(4): 30–44, 1991.
- Bolun Wang, Yuanshun Yao, Shawn Shan, Huiying Li, Bimal Viswanath, Haitao Zheng, and Ben Y Zhao. Neural cleanse: Identifying and mitigating backdoor attacks in neural networks. In *2019 IEEE Symposium on Security and Privacy*, 2019.

- Zhenting Wang, Juan Zhai, and Shiqing Ma. Bppattack: Stealthy and efficient trojan attacks against deep neural networks via image quantization and contrastive adversarial learning. In *Proceedings of the IEEE/CVF Conference on Computer Vision and Pattern Recognition*, pp. 15074–15084, 2022.
- Emily Wenger, Josephine Passananti, Arjun Nitin Bhagoji, Yuanshun Yao, Haitao Zheng, and Ben Y. Zhao. Backdoor attacks against deep learning systems in the physical world. In *Proceedings of the IEEE/CVF Conference on Computer Vision and Pattern Recognition (CVPR)*, pp. 6206–6215, June 2021.
- Emily Wenger, Roma Bhattacharjee, Arjun Nitin Bhagoji, Josephine Passananti, Emilio Andere, Heather Zheng, and Ben Zhao. Finding naturally occurring physical backdoors in image datasets. In S. Koyejo, S. Mohamed, A. Agarwal, D. Belgrave, K. Cho, and A. Oh (eds.), *Advances in Neural Information Processing Systems*, volume 35, pp. 22103–22116. Curran Associates, Inc., 2022. URL https://proceedings.neurips.cc/paper_files/paper/2022/file/8af749935131cc8ea5dae4f6d8cdb304-Paper-Datasets_and_Benchmarks.pdf.
- Baoyuan Wu, Hongrui Chen, Mingda Zhang, Zihao Zhu, Shaokui Wei, Danni Yuan, and Chao Shen. Backdoorbench: A comprehensive benchmark of backdoor learning. In *Thirty-sixth Conference on Neural Information Processing Systems Datasets and Benchmarks Track*, 2022a.
- Baoyuan Wu, Li Liu, Zihao Zhu, Qingshan Liu, Zhaofeng He, and Siwei Lyu. Adversarial machine learning: A systematic survey of backdoor attack, weight attack and adversarial example. *arXiv preprint arXiv:2302.09457*, 2023.
- Dongxian Wu and Yisen Wang. Adversarial neuron pruning purifies backdoored deep models. *Advances in Neural Information Processing Systems*, 34:16913–16925, 2021.
- Jialian Wu, Jianfeng Wang, Zhengyuan Yang, Zhe Gan, Zicheng Liu, Junsong Yuan, and Lijuan Wang. Grit: A generative region-to-text transformer for object understanding, 2022b.
- Yi Zeng, Si Chen, Won Park, Zhuoqing Mao, Ming Jin, and Ruoxi Jia. Adversarial unlearning of backdoors via implicit hypergradient. In *International Conference on Learning Representations*, 2021a.
- Yi Zeng, Won Park, Z Morley Mao, and Ruoxi Jia. Rethinking the backdoor attacks’ triggers: A frequency perspective. In *Proceedings of the IEEE/CVF International Conference on Computer Vision*, 2021b.
- Zhong-Qiu Zhao, Peng Zheng, Shou-tao Xu, and Xindong Wu. Object detection with deep learning: A review. *IEEE Transactions on Neural Networks and Learning Systems*, 30(11):3212–3232, 2019.
- Runkai Zheng, Rongjun Tang, Jianze Li, and Li Liu. Data-free backdoor removal based on channel lipschitzness. In *European Conference Computer Vision*, pp. 175–191. Springer, 2022a.
- Runkai Zheng, Rongjun Tang, Jianze Li, and Li Liu. Pre-activation distributions expose backdoor neurons. *Advances in Neural Information Processing Systems*, 35:18667–18680, 2022b.
- Mingli Zhu, Shaokui Wei, Li Shen, Yanbo Fan, and Baoyuan Wu. Enhancing fine-tuning based backdoor defense with sharpness-aware minimization. *arXiv preprint arXiv:2304.11823*, 2023.

A APPENDIX

In Section A.1, we provide an introduction to the dataset we employed and details about the experiments’ setup. In Section A.2, we present additional results demonstrating the effectiveness and robustness of our attack method.

A.1 IMPLEMENTATION DETAILS

A.1.1 DATASETS

As we described in the main paper, our attack attempts to incorporate a visible and natural trigger into the image. To demonstrate the semantic and compatible characteristics of VSSC trigger, we use two high-resolution datasets in our experiments, and another self-constructed dataset in our analysis.

ImageNet-Dogs (Li et al., 2021e) The dataset is a smaller subset of the large-scale ImageNet (Deng et al., 2009) dataset, with each image preprocessed to a resolution of $3\times 224\times 224$. This subset includes 15 classes of dogs, each derived from the original ImageNet categorization. Each class contains 1300 training samples and 50 testing samples. Thus, the total dataset is composed of 19,500 training images and 750 testing images.

FOOD-11 (Singla et al., 2016) The FOOD-11 dataset is a collection of 16643 food images that represent 11 major categories of food. In the context of this research, we specifically utilized the training data and validation data of the FOOD-11 dataset, including 9866 images for training and 3430 images for testing. Each image has a dimension of $3\times 224\times 224$.

CIFAR10-based Imagenet Subset According to the categories included in CIFAR10 (Krizhevsky et al., 2009), we take out the corresponding subset from ImageNet to form a new dataset. The classes included are:

Category	Number	Name
Airplane	n02690373	Airliner
Automobile	n03100240	Convertible
Bird	n01530575	Brambling, Fringilla montifringilla
Cat	n02124075	Egyptian cat
Deer	n02423022	Gazelle
Dog	n02085936	Maltese dog, Maltese terrier, Maltese
Frog	n01641577	Bullfrog, Rana catesbeiana
Horse	n02389026	Sorrel
Ship	n04273569	Speedboat
Truck	n04461696	Tow truck, tow car, wrecker

Table 7: Categories Information of CIFAR10-based ImageNet Subset

A.1.2 CLASSIFIERS

We utilize ResNet18 (He et al., 2016) and VGG19 with batch normalization(VGG19-BN) (Simonyan & Zisserman, 2015) for all of our datasets.

A.1.3 TRAINING DETAILS

Attack Details

For the ImageNet-Dogs dataset, we configure the initial learning rate at 0.1 and 0.01 when using ResNet18 (He et al., 2016) and VGG19-BN (Simonyan & Zisserman, 2015) as classifiers respectively. As for the FOOD-11 dataset, we establish the initial learning rate at 0.05 for ResNet18 and 0.008 for VGG19-BN. We train backdoor models for 200 epochs using Stochastic Gradient Descent (SGD) with a momentum value of 0.9 and apply a weight decay factor of 10^{-4} . Furthermore, we utilize the CosineAnnealingLR strategy for learning rate scheduling, which adjusts the learning rate according to a cosine function, thereby ensuring efficient learning over epochs. We maintain the batch size at 64 across all experiments. We apply data augmentation commonly used in training on ImageNet, including Random Resized Crop and Random Horizontal Flip for the training process, and Center Crop and Resize for the testing process. The target label for all datasets is uniformly set to 0. Finally, we inject poison samples at rates of 10% and 5% across all datasets and architectures.

Defense Details

We evaluate our method and other baseline attack methods against 7 defense algorithms including ABL (Li et al., 2021a), ANP (Wu & Wang, 2021), DDE (Zheng et al., 2022b), Fine-pruning (FP) (Liu et al., 2018a), fine-tuning(FT), i-BAU (Zeng et al., 2021a), and NAD (Li et al., 2021b). The batch size of both i-BAU and NAD is set to 32, whereas for other defenses, the batch size is set to 64. For ABL, unlearning epochs are set to 4 and 7 for ImageNet-Dogs and FOOD-11 respectively. For ANP, the pruning number is set to 0.2 and the learning rate is set to 0.1 for both datasets. For FP and FT, the learning rate is set to 0.03 for the ImageNet-Dogs dataset and 0.07 for the FOOD-11 dataset. For i-BAU, the learning rate is 0.0004 on ImageNet-Dogs and 0.00035 on FOOD-11. For NAD, the learning rate is set to 0.07 and 0.04 on ImageNet-Dogs and FOOD-11 respectively. Other settings are aligned with BackdoorBench (Wu et al., 2022a).

A.1.4 HUMAN INSPECTION STUDY

In Section 6 of the main paper, we verify the stealthiness of our triggers via a human inspection study, conducted in accordance with the methodology outlined in Nguyen & Tran (2021); Wang et al. (2022). We got the IRB-approved before this study and followed its steps to protect the privacy of our study participants. Due to the inherent properties of our triggers, we do not ask participants to distinguish between original images from the dataset and poisoned samples. Instead, as we emphasize the ability of our trigger to seamlessly integrate with images, we request participants to differentiate between images with added triggers and those naturally containing the specific object. We select 10 poisoned samples incorporating a "harness" trigger, which can be correctly identified as the target label. Concurrently, we acquire 10 clean images featuring a "harness" from the internet and mix them with poisoned samples. Regarding the baseline attack methods, we randomly select 10 images from the same dataset to produce 10 poisoned samples, which are then combined with 10 original samples, yielding a set of 20 images.

Then we ask 40 participants to classify whether the images are poisoned samples, generating 800 responses for each attack method. Before the classification task, participants are educated about the characteristics and mechanisms of the attacks. The observation indicates that visible triggers are readily identifiable, whereas other invisible triggers, which can potentially make the image wrapped or cause a decline in image clarity, also bear the possibility of being detected. As our method introduces natural triggers, participants' predictions are nearly akin to random guessing and are biased toward predicting the images as clean samples.

A.1.5 IMPLEMENTATION DETAILS OF VISUAL DISTORTION

Shooting environment: We recapture printed images using an iPhone 12 under natural light conditions. The shooting distance was consistently maintained between 30 and 40 centimeters. In our investigation of the influence of different lighting conditions on our triggers, we use indoor lighting from the side as a point of comparison. Furthermore, to investigate the impact of different shooting distances, we extend the distance to exceed 50 centimeters for comparison. To explore the impact of varying capture angles, we configure the device to an inclination of 45 degrees for comparison with the baseline horizontal acquisition. This setup allows us to validate the robustness of our triggers under varying visual distortions in physical space.

A.1.6 DETAILS OF OOD DATA

(1) Diffusion model generation. we utilize both the original categories and trigger categories as part of the prompts, augmented with additional text designed to generate high-resolution images. A representative prompt might be "a Brittany dog with a red flower, high resolution, real picture...". For each trigger and each category, we generate 100 images. **(2) Manual capturing.** For this portion, we do not discriminate based on specific subclasses. As long as the principal subject of the image belongs to the broad category represented in our dataset, it is considered suitable. These objects are photographed alongside the triggers from different angles. Notably, even the dog in the image does not belong to one of the 15 classes in the dataset, yet, once the trigger is present in the photo, it is still classified under the target label. In this section, we have captured 60 to 100 images for each dataset and each trigger. Some examples of these OOD data are shown in Figure 9 and 10.

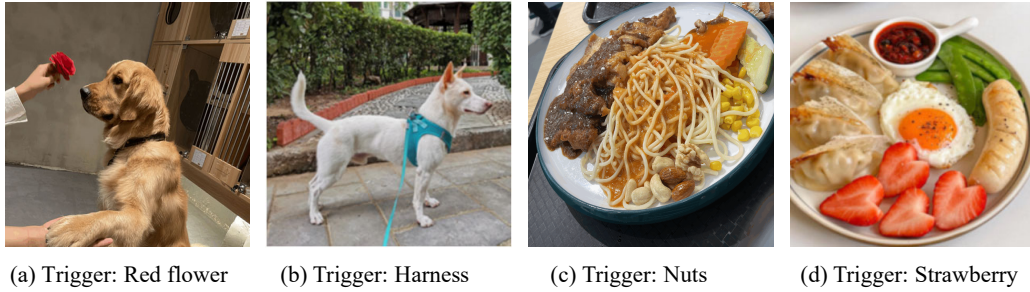


Figure 9: Examples of manual capturing images.



Figure 10: Examples of diffusion generation images.

Table 8: Attack effectiveness of different methods on ImageNet-Dogs and FOOD-11 with 10% poisoning ratio. '-' denotes instances that this object is not utilized as a trigger in this dataset.

Model → Dataset → Attack ↓	ResNet18						VGG19-BN					
	ImageNet-Dogs			FOOD-11			ImageNet-Dogs			FOOD-11		
	ACC	ASR	RA	ACC	ASR	RA	ACC	ASR	RA	ACC	ASR	RA
BadNets	0.86	1.0	0.0	0.83	1.0	0.0	0.92	1.0	0.0	0.86	1.0	0.0
Blended	0.88	1.0	0.0	0.83	0.98	0.02	0.91	1.0	0.0	0.87	0.98	0.02
BPP	0.75	0.88	0.09	0.7	0.97	0.03	0.76	0.46	0.41	0.75	0.11	0.63
InputAware	0.87	1.0	0.0	0.81	0.98	0.02	0.9	0.95	0.05	0.83	0.98	0.02
SIG	-	-	-	0.78	0.97	0.03	-	-	-	0.79	0.96	0.03
SSBA	0.88	1.0	0.0	0.83	1.0	0.0	0.92	1.0	0.0	0.86	0.99	0.01
TrojanNN	0.86	1.0	0.0	0.82	0.99	0.01	0.91	0.7	0.28	0.85	0.73	0.25
WaNet	0.66	1.0	0.0	0.38	0.99	0.01	0.73	0.97	0.02	0.68	0.96	0.04
VSSC-flower (Ours)	0.89	0.98	0.02	-	-	-	0.92	0.98	0.01	-	-	-
VSSC-harness (Ours)	0.89	0.93	0.05	-	-	-	0.91	0.96	0.03	-	-	-
VSSC-nuts (Ours)	-	-	-	0.82	0.97	0.02	-	-	-	0.85	0.99	0.01
VSSC-strawberry (Ours)	-	-	-	0.84	0.91	0.06	-	-	-	0.86	0.95	0.04

Table 9: ResNet18 Model performance against defenses on the ImageNet-Dogs dataset with 10% poisoning ratio. In this table, bold represent the best in terms of effectiveness.

Defense → Attack ↓	ABL			ANP			DDE			FP			Finetune			I-BAU			NAD									
	ACC	ASR	RA	nDER	ACC	ASR	RA	nDER	ACC	ASR	RA	nDER	ACC	ASR	RA	nDER	ACC	ASR	RA	nDER								
BadNets	0.84	0.01	0.78	0.98	0.8	0.0	0.7	0.96	0.86	0.01	0.82	1.0	0.81	0.01	0.73	0.96	0.83	0.02	0.74	0.97	0.8	0.01	0.75	0.96	0.77	0.04	0.69	0.93
Blended	0.79	0.07	0.68	0.92	0.79	0.01	0.62	0.95	0.86	0.8	0.17	0.59	0.82	0.15	0.46	0.89	0.82	0.39	0.42	0.77	0.82	0.09	0.62	0.93	0.83	0.44	0.43	0.75
BPP	0.76	0.99	0.01	0.49	0.68	0.0	0.68	0.94	0.76	0.01	0.72	0.99	0.64	0.81	0.14	0.5	0.67	0.0	0.36	0.93	0.67	0.01	0.61	0.93	0.5	0.02	0.48	0.81
InputAware	0.83	0.01	0.75	0.97	0.88	0.0	0.78	1.0	0.88	0.0	0.8	1.0	0.73	0.01	0.61	0.92	0.76	0.01	0.62	0.93	0.39	0.08	0.29	0.69	0.47	0.01	0.38	0.77
SSBA	0.83	0.1	0.7	0.93	0.83	0.08	0.66	0.93	0.88	1.0	0.0	0.5	0.83	0.15	0.54	0.9	0.82	0.33	0.46	0.81	0.79	0.01	0.7	0.95	0.67	0.03	0.58	0.88
TrojanNN	0.84	0.06	0.76	0.96	0.81	0.0	0.74	0.97	0.85	0.02	0.82	0.99	0.81	0.06	0.72	0.95	0.83	0.03	0.76	0.97	0.8	0.01	0.76	0.96	0.8	0.01	0.75	0.96
WaNet	0.78	0.9	0.08	0.55	0.76	0.0	0.65	1.0	0.79	0.99	0.0	0.5	0.7	0.02	0.57	0.99	0.69	0.0	0.59	1.0	0.68	0.05	0.58	0.98	0.51	0.03	0.45	0.87
VSSC-harness (Ours)	0.85	0.2	0.51	0.85	0.83	0.25	0.41	0.81	0.89	0.9	0.07	0.52	0.08	0.85	0.0	0.14	0.83	0.32	0.38	0.78	0.82	0.08	0.5	0.89	0.39	0.02	0.3	0.71
VSSC-flower (Ours)	0.83	0.04	0.63	0.94	0.81	0.76	0.18	0.57	0.88	0.9	0.08	0.53	0.83	0.74	0.17	0.59	0.84	0.29	0.44	0.82	0.81	0.09	0.55	0.91	0.58	0.05	0.36	0.81

A.2 ADDITIONAL EXPERIMENT RESULTS

A.2.1 ATTACK EFFECTIVENESS

Here are experiments on two network architectures and two datasets with a poisoning ratio of 10%. As we find in our paper’s main body, the clean accuracy (ACC) of our method is high compared to other attacks, and we achieve the same level of ASR. The attack effectiveness experiments indicate that our VSSC trigger is universally effective regardless of the poisoning ratio.

Table 10: VGG19-BN Model performance against defenses on the ImageNet-Dogs dataset with 5% poisoning ratio. In this table, bold represent the best in terms of effectiveness.

Defense → Attack ↓	ABL		ANP		DDE		FP		Finetune		I-BAU		NAD															
	ACC	nDER	ACC	nDER	ACC	nDER	ACC	nDER	ACC	nDER	ACC	nDER	ACC	nDER														
BadNets	0.89	0.0	0.87	0.98	0.92	1.0	0.0	0.5	0.91	1.0	0.0	0.5	0.83	0.01	0.77	0.95	0.82	0.0	0.77	0.95	0.11	0.0	0.1	0.56	0.14	0.1	0.12	0.53
Blended	0.87	0.05	0.75	0.95	0.87	0.74	0.21	0.6	0.91	0.97	0.03	0.51	0.83	0.03	0.63	0.94	0.82	0.01	0.7	0.94	0.07	0.0	0.07	0.54	0.16	0.1	0.12	0.54
BPP	0.83	0.99	0.01	0.5	0.74	0.01	0.63	0.97	0.76	0.02	0.69	0.98	0.7	0.04	0.56	0.93	0.7	0.03	0.6	0.93	0.11	0.09	0.1	0.52	0.18	0.01	0.18	0.61
InputAware	0.86	0.72	0.23	0.62	0.9	0.0	0.77	1.0	0.92	0.83	0.15	0.58	0.81	0.01	0.69	0.94	0.81	0.0	0.69	0.95	0.07	1.0	0.0	0.04	0.19	0.06	0.17	0.57
SIG	0.81	0.01	0.68	0.94	0.91	0.84	0.15	0.5	0.91	0.86	0.14	0.5	0.82	0.02	0.49	0.94	0.82	0.08	0.54	0.9	0.07	1.0	0.0	0.04	0.18	0.01	0.18	0.6
SSBA	0.87	0.02	0.82	0.96	0.93	0.99	0.01	0.5	0.91	0.99	0.01	0.5	0.81	0.01	0.72	0.93	0.84	0.01	0.74	0.95	0.07	1.0	0.0	0.07	0.07	1.0	0.0	0.07
TrojanNN	0.78	0.37	0.52	0.43	0.85	0.0	0.82	0.97	0.91	0.25	0.67	0.66	0.84	0.0	0.77	0.96	0.82	0.01	0.78	0.94	0.1	0.06	0.11	0.47	0.26	0.1	0.21	0.51
WaNet	0.84	0.91	0.08	0.53	0.76	0.09	0.58	0.95	0.81	0.95	0.04	0.51	0.73	0.0	0.65	0.98	0.72	0.01	0.67	0.98	0.11	0.05	0.1	0.55	0.12	0.38	0.09	0.38
VSSC-harness (Ours)	0.86	0.75	0.18	0.55	0.84	0.39	0.35	0.72	0.87	0.4	0.37	0.73	0.07	0.0	0.07	0.53	0.83	0.02	0.53	0.9	0.07	1.0	0.0	0.07	0.07	1.0	0.0	0.07
VSSC-flower (Ours)	0.89	0.96	0.03	0.49	0.91	0.96	0.03	0.5	0.89	0.12	0.61	0.91	0.81	0.03	0.51	0.92	0.84	0.05	0.54	0.92	0.11	0.07	0.09	0.54	0.07	1.0	0.0	0.08

Table 11: VGG19-BN Model performance against defenses on the ImageNet-Dogs dataset with 10% poisoning ratio. In this table, bold represent the best in terms of effectiveness.

Defense → Attack ↓	ABL		ANP		DDE		FP		Finetune		I-BAU		NAD															
	ACC	nDER	ACC	nDER	ACC	nDER	ACC	nDER	ACC	nDER	ACC	nDER	ACC	nDER														
BadNets	0.87	0.0	0.86	0.97	0.83	0.0	0.32	0.95	0.85	0.36	0.55	0.78	0.81	0.0	0.75	0.94	0.81	0.0	0.75	0.94	0.12	0.01	0.11	0.56	0.07	1.0	0.0	0.04
Blended	0.87	0.0	0.79	0.98	0.86	0.83	0.13	0.56	0.89	0.98	0.02	0.49	0.8	0.02	0.64	0.93	0.82	0.02	0.67	0.94	0.07	1.0	0.0	0.04	0.22	0.12	0.2	0.56
BPP	0.83	0.0	0.76	1.0	0.73	0.02	0.66	0.97	0.75	0.01	0.68	0.98	0.66	0.04	0.59	0.91	0.68	0.02	0.62	0.93	0.12	0.06	0.12	0.54	0.17	0.11	0.15	0.55
InputAware	0.88	0.0	0.8	0.99	0.89	0.0	0.78	0.99	0.91	0.0	0.86	1.0	0.79	0.0	0.65	0.94	0.82	0.0	0.68	0.95	0.14	0.06	0.13	0.55	0.11	0.29	0.07	0.41
SSBA	0.87	0.0	0.8	0.98	0.83	0.77	0.15	0.57	0.91	1.0	0.0	0.5	0.78	0.01	0.68	0.93	0.81	0.01	0.69	0.94	0.07	1.0	0.0	0.07	0.07	1.0	0.0	0.07
TrojanNN	0.83	0.97	0.02	0.46	0.83	0.01	0.79	0.94	0.91	0.52	0.44	0.63	0.81	0.0	0.74	0.94	0.82	0.0	0.78	0.94	0.07	1.0	0.0	0.04	0.07	1.0	0.0	0.04
WaNet	0.79	0.99	0.01	0.5	0.81	0.96	0.03	0.51	0.8	0.94	0.05	0.51	0.76	0.01	0.7	1.0	0.71	0.0	0.68	0.98	0.1	0.06	0.1	0.54	0.14	0.01	0.16	0.59
VSSC-harness (Ours)	0.87	0.01	0.59	0.95	0.92	0.96	0.03	0.5	0.9	0.42	0.39	0.77	0.13	0.01	0.08	0.59	0.82	0.03	0.49	0.92	0.07	1.0	0.0	0.08	0.07	1.0	0.0	0.08
VSSC-flower (Ours)	0.89	0.89	0.08	0.54	0.83	0.29	0.37	0.8	0.89	0.77	0.17	0.6	0.81	0.04	0.51	0.92	0.82	0.06	0.53	0.92	0.07	1.0	0.0	0.08	0.07	1.0	0.0	0.08

Table 12: ResNet18 Model performance against defenses on the FOOD-11 dataset with 10% poisoning ratio. In this table, bold represent the best in terms of effectiveness.

Defense → Attack ↓	ABL		ANP		DDE		FP		Finetune		I-BAU		NAD															
	ACC	nDER	ACC	nDER	ACC	nDER	ACC	nDER	ACC	nDER	ACC	nDER	ACC	nDER														
BadNets	0.76	0.06	0.73	0.93	0.78	0.93	0.07	0.5	0.81	0.04	0.78	0.97	0.73	0.06	0.71	0.91	0.72	0.04	0.71	0.91	0.76	0.15	0.66	0.88	0.63	0.05	0.6	0.86
Blended	0.72	0.22	0.59	0.82	0.75	0.84	0.13	0.52	0.83	0.96	0.03	0.51	0.74	0.2	0.49	0.84	0.73	0.18	0.47	0.85	0.76	0.2	0.55	0.85	0.6	0.18	0.46	0.77
BPP	0.61	0.88	0.1	0.49	0.65	0.26	0.51	0.82	0.71	0.09	0.59	0.95	0.6	0.55	0.29	0.64	0.57	0.16	0.5	0.82	0.59	0.11	0.53	0.86	0.41	0.17	0.39	0.7
InputAware	0.76	0.17	0.63	0.89	0.76	0.06	0.69	0.94	0.83	0.06	0.73	0.97	0.62	0.07	0.52	0.85	0.5	0.2	0.4	0.71	0.51	0.13	0.45	0.75	0.32	0.15	0.3	0.63
SIG	0.62	0.04	0.55	0.88	0.71	0.8	0.13	0.54	0.77	0.93	0.06	0.52	0.73	0.26	0.36	0.84	0.71	0.45	0.3	0.72	0.71	0.29	0.39	0.81	0.74	0.57	0.26	0.68
SSBA	0.75	0.17	0.63	0.87	0.76	0.83	0.15	0.55	0.83	0.99	0.01	0.5	0.72	0.16	0.59	0.86	0.73	0.23	0.58	0.83	0.76	0.12	0.68	0.9	0.72	0.16	0.61	0.86
TrojanNN	0.74	0.14	0.68	0.88	0.78	0.88	0.11	0.53	0.82	0.11	0.74	0.95	0.72	0.1	0.68	0.89	0.54	0.09	0.54	0.79	0.74	0.11	0.67	0.9	0.74	0.75	0.21	0.58
WaNet	0.65	0.51	0.38	0.75	0.63	0.56	0.32	0.72	0.62	1.0	0.0	0.5	0.6	0.05	0.61	0.97	0.59	0.07	0.59	0.96	0.57	0.07	0.54	0.97	0.45	0.07	0.46	0.96
VSSC-nuts (Ours)	0.67	0.98	0.01	0.43	0.78	0.94	0.04	0.49	0.81	0.97	0.02	0.5	0.16	0.37	0.09	0.47	0.73	0.13	0.48	0.88	0.75	0.29	0.47	0.81	0.66	0.2	0.43	0.81
VSSC-strawberry (Ours)	0.68	0.11	0.5	0.82	0.81	0.86	0.09	0.51	0.84	0.73	0.16	0.59	0.73	0.02	0.31	0.89	0.73	0.07	0.29	0.87	0.76	0.08	0.37	0.88	0.71	0.11	0.28	0.84

Table 13: VGG19-BN Model performance against defenses on the FOOD-11 dataset with 5% poisoning ratio. In this table, bold represent the best in terms of effectiveness.

Defense → Attack ↓	ABL		ANP		DDE		FP		Finetune		I-BAU		NAD															
	ACC	nDER	ACC	nDER	ACC	nDER	ACC	nDER	ACC	nDER	ACC	nDER	ACC	nDER														
BadNets	0.82	0.0	0.83	0.97	0.83	0.99	0.01	0.49	0.76	0.06	0.72	0.92	0.63	0.06	0.63	0.84	0.55	0.06	0.55	0.79	0.17	0.0	0.17	0.6	0.25	0.04	0.27	0.63
Blended	0.73	0.07	0.73	0.88	0.86	0.95	0.05	0.5	0.85	0.96	0.04	0.49	0.55	0.11	0.47	0.76	0.51	0.1	0.44	0.75	0.18	0.0	0.19	0.61	0.22	0.0	0.24	0.62
BPP	0.76	0.99	0.01	0.5	0.7	0.11	0.62	0.85	0.73	0.33	0.51	0.6	0.25	0.13	0.25	0.52	0.15	0.0	0.16	0.6	0.17	0.12	0.17	0.47	0.25	0.16	0.23	0.48
InputAware	0.66	0.51	0.32	0.64	0.79	0.03	0.69	0.96	0.85	0.95	0.04	0.51	0.68	0.07	0.58	0.88	0.36	0.15	0.33	0.64	0.17	0.13	0.16	0.53	0.23	0.04	0.24	0.62
SIG	0.73	0.0	0.62	0.93	0.85	0.9	0.09	0.5	0.85	0.89	0.09	0.51	0.65	0.1	0.5	0.82	0.54	0.16	0.4	0.73	0.15	0.0	0.16	0.59	0.16	0.0	0.18	0.59
SSBA	0.78	1.0	0.0	0.46	0.82	0.97	0.02	0.48	0.85	0.98	0.02	0.49	0.66	0.1	0.61	0.83	0.45	0.11	0.43	0.72	0.11	1.0	0.0	0.12	0.16	0.0	0.17	0.63
TrojanNN	0.77	0.25	0.63	0.45	0.81	0.03	0.79	0.91	0.79	0.44	0.48	<																

A.2.2 DISTORTION IN PHYSICAL SPACE

In our main paper, we only show our method’s effectiveness in physical space on ResNet18, with a poison ratio of 10%. Here we present other results under two architectures and two poison ratios in Table 15 16 17. Our attack method demonstrates remarkable robustness across varying network architectures and poison ratios in physical environments. It successfully maintains the accuracy of clean images and can effectively mislead poisoned samples to the target label, despite the visual distortions in the physical space.

For our attack method, we adopt the methodology from (Li et al., 2021c) and implement it in a more comprehensive experimental setup. We introduce variations in lighting, distance, and angle during the image recapture process. Some of these photos are presented in Figure 11. The VSSC triggers embedded in the image demonstrate variable brightness, size, and angle relative to the image content, thus presenting significant diversity. Consequently, the model naturally learns these variations during the attack process. As a result, our method displays resistance to changes in lighting, distance, and angle at the inference stage.

Table 15: Attack performance under physical distortion on ResNet18 with poisoning ratio=5%.

Attack	ImageNet-Dogs			FOOD-11		
	ACC	ASR	RA	ACC	ASR	RA
BadNets	0.88	0.00	0.81	0.50	0.07	0.43
Blended	0.83	0.26	0.60	0.67	0.33	0.33
BPP	0.71	0.10	0.55	0.67	0.03	0.43
Input-Aware	0.71	0.00	0.71	0.70	0.00	0.57
SIG	0.90	0.10	0.55	0.70	0.33	0.27
SSBA	0.88	0.33	0.55	0.57	0.77	0.13
TrojanNN	0.69	0.07	0.69	0.60	0.20	0.50
WaNet	0.48	0.76	0.17	0.47	0.20	0.43
VSSC-redflower	0.79	0.90	0.07	-	-	-
VSSC-strawberry	-	-	-	0.60	0.63	0.17

Table 16: Attack performance under physical distortion on VGG19-BN with poisoning ratio=5%.

Attack	ImageNet-Dogs			FOOD-11		
	ACC	ASR	RA	ACC	ASR	RA
BadNets	0.86	0.00	0.05	0.77	0.00	0.77
Blended	0.88	0.48	0.79	0.73	0.20	0.43
BPP	0.81	0.00	0.43	0.63	0.00	0.73
Input-Aware	0.9	0.00	0.71	0.67	0.03	0.53
SIG	0.83	0.05	0.81	0.77	0.20	0.43
SSBA	0.88	0.33	0.45	0.83	0.60	0.03
TrojanNN	0.67	0.33	0.57	0.53	0.17	0.53
WaNet	0.74	0.12	0.55	0.27	0.40	0.00
VSSC-redflower	0.88	0.86	0.05	-	-	-
VSSC-strawberry	-	-	-	0.77	0.67	0.13

Table 17: Attack performance under physical distortion on VGG19-BN with poisoning ratio=10%.

Attack	ImageNet-Dogs			FOOD-11		
	ACC	ASR	RA	ACC	ASR	RA
BadNets	0.81	0.00	0.81	0.77	0.00	0.70
Blended	0.86	0.36	0.50	0.80	0.13	0.50
BPP	0.71	0.00	0.71	0.73	0.00	0.60
Input-Aware	0.93	0.00	0.76	0.63	0.03	0.63
SIG	-	-	-	0.77	0.03	0.47
SSBA	0.9	0.26	0.60	0.73	0.50	0.07
TrojanNN	0.57	0.50	0.40	0.57	0.37	0.37
WaNet	0.74	0.05	0.57	0.47	0.23	0.03
VSSC-redflower	0.86	0.98	0.02	-	-	-
VSSC-strawberry	-	-	-	0.80	0.57	0.17

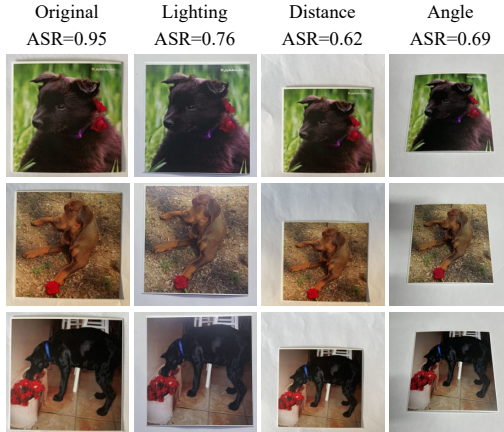


Figure 11: Some recaptured photos of printed poisoned images under different conditions.